University of Groningen

Hollow-cathode activated PECVD for the high-rate deposition of permeation barrier films

Top, Michiel; Schoenfeld, Steffen; Fahlteich, John; Bunk, Sebastian; Kuehnel, Thomas; Straach, Steffen; De Hosson, Jeff T.

IMPORTANT NOTE: You are advised to consult the publisher's version (publisher's PDF) if you wish to cite from it. Please check the document version below.

Document Version
Publisher's PDF, also known as Version of record

[Link to publication in University of Groningen/UMCG research database](#)

CrossMark

Hollow-cathode activated PECVD for the high-rate deposition of permeation barrier films

Michiel Top [a,b,*], Steffen Schönfeld [a], John Fahlteich [a], Sebastian Bunk [a], Thomas Kühnel [a], Steffen Straach [a], Jeff T. De Hosson [b]

[a] *Fraunhofer Institute for Organic Electronics, Electron Beam and Plasma Technology FEP, Winterbergstrasse 28, 01277 Dresden, Germany*
[b] *Department of Applied Physics, University of Groningen, Nijenborgh 4, 9747, AG, Groningen, The Netherlands*

ABSTRACT

This paper shows a study on the variation of the flow ratio between oxygen and Hexamethyldisiloxane (HMDSO) in a hollow cathode arc PECVD process. Dynamic deposition rates were measured between 300 and 500 nm ∗ m/min. The deposited plasma polymer films were analyzed using visible light spectroscopy, X-ray photo-electron spectroscopy (XPS), X-ray reflectivity (XRR), Fourier-transformed infrared spectroscopy (FTIR), Scanning electron microscopy (SEM) and water vapor transmission rate (WVTR) measurements. The deposited samples were compared to a reactively sputtered SiO_2 thin film. By increasing the oxygen to HMDSO flow ratio, the chemical, density and optical properties of the coating approached the sputtered SiO_2 film. However the permeation barrier of the SiO_2 film only shows a slight improvement over that of the bare PET substrate. The organic coating with high power and low oxygen flow, which was deposited with a deposition rate of 450 nm ∗ m/min, approached the barrier of the sputtered SiO_2 thin film with a WVTR of 0.16 g/(m^2 day).

© 2016 Elsevier B.V. All rights reserved.

1. Introduction

To increase the lifetime of food and drinks, most food packaging materials are provided with a barrier layer which reduces the permeation of water and oxygen through the film. Apart from food packaging there is an upcoming market for ultra-high barrier films which are used for the encapsulation of organic electronics [1]. A common barrier material with good barrier but also great optical properties is SiO_2 [2–4].

These inorganic barrier layers are commonly deposited using electron beam evaporation [5], reactive sputtering [6,7], plasma enhanced chemical vapor deposition (PECVD) [2,8–10], or Atomic Layer Deposition (ALD) [11], whereas electron beam evaporation is a high rate technique, the latter techniques are usually low rate but have less defects. PECVD has advantages over the other techniques due to its low heat load to the substrate [12] and good mechanical properties resulting in higher cracking resistance [13]. Another advantage is the ability to easily influence the chemical composition, by changing the used gases and their composition within the deposition chamber. This allows the deposition of both inorganic as well as organic coatings.

A lot of research has been devoted to the deposition of SiO_x layers using PECVD. In general, an RF (13.56 MHz) or microwave source is used to generate a glow discharge plasma. For the deposition of silica containing films, the monomer HMDSO can be used as a monomer. Oxygen is added as a reactive gas. Changing the Oxygen/HMDSO ratio influences the organic character of the deposited layers. Several authors showed that the permeation of water and oxygen decrease with increasing oxygen flow. [2,14,15]. However, Bieder et al. [2] observed, when using a dual mode plasma with MW and RF, an increased WVTR for O_2/HMDSO ratios above 20.

Several researchers investigated the chemical and interfacial properties of $SiO_xC_yH_z$ layers deposited using different types of plasma [16–18]. However, no comparison was made to the chemical structure of inorganic reactively sputtered SiO_2 which is known for being a good barrier material. In this paper, a hollow cathode plasma source was operated in the DC arc discharge mode while injecting oxygen and evaporated HMDSO to deposited silicon containing plasma polymers in a high-rate roll to roll process on a PET substrate. The chemical and barrier properties as well as the mass density of these samples were compared to a sputtered SiO_2 layer [6].

2. Experimental setup

The plasma polymer coatings were deposited in the roll-to-roll web coater novoFlex® 600. More information about the novoFlex® 600 can be found elsewhere [19,20]. The hollow cathodes were used to create a

* Corresponding author at: Fraunhofer Institute for Organic Electronics, Electron Beam and Plasma Technology FEP, Winterbergstrasse 28, 01277 Dresden, Germany.
E-mail addresses: michiel.top@fep.fraunhofer.de (M. Top),
john.fahlteich@fep.fraunhofer.de (J. Fahlteich), Sebastian.bunk@fep.fraunhofer.de
(S. Bunk), Thomas.kuehnel@fep.fraunhofer.de (T. Kühnel),
steffen.straach@fep.fraunhofer.de (S. Straach), J.T.M.De.Hosson@rug.nl (J.T. De Hosson).
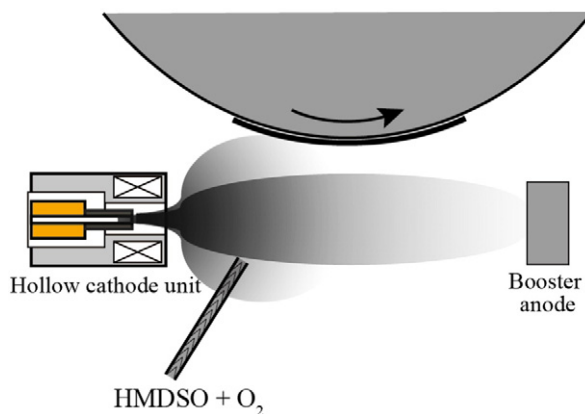
Fig. 1. A schematic representation of the deposition geometry in the novoFlex® 600. Hollow cathode unit contains the cathode as well as the annular anode.

dense plasma that fragmentizes and ionizes the HMDSO and oxygen. The setup is shown in Fig. 1. On the left, the hollow cathode is shown. Argon is injected through the hollow cathode. The hollow cathode is equipped with two anodes. The first one is the so-called primary anode, which is an annular anode directly mounted around the cathode. It is mainly used during the initiation of the plasma and to create a dense plasma around the outlet of the cathode. The booster anode is used to create a dense plasma around the gas inlets. Both anodes are powered by two separate current sources. Oxygen and HMDSO are purged into the plasma using metal tubes. Within the novoFlex® 600, the coating width goes up to 600 mm. Therefore, the systems is equipped with 4 hollow cathodes in a row, 9 booster anodes and 12 gas inlets to allow for deposition over the full web-width. A constant HMDSO flow of 125 sccm was used for all experiments whereas the oxygen flow was adjusted to obtain the oxygen to HMDSO ratio. The current of the booster anode was set to 17 A and 34 A. Further increase of the current was not possible due to the limited thermal load that the polymer substrate can withstand. From now on, the first sample series will be referred to as low power and the latter to as high power. Further process parameters are given in Table 1. The process pressure was measured between 0.1 and 0.4 Pa depending on the oxygen flow.

The sputtered SiO_2 layer is deposited in the labFlex® 200 web coater using reactive dual magnetron sputtering. More info about this technique is described elsewhere [21]. All samples were deposited on a 75 μm thick Polyethylene terephthalate (PET) substrate (Melinex 401 CW, DuPont Teijin Films).

After the deposition, the barrier and chemical properties of the thin film coatings were analyzed. A L900 optical spectrometer (Perkin Elmer) was used to measure the transmission spectra of the samples between 300 and 1300 nm. The thickness was calculated by simulation of

Table 1
Deposition parameters that were used for the deposition. For parameters that were varied, the range is given.

Process parameter	Range
Web speed	1 m/min
Cooling drum temperature	0 °C
Argon flow	500 sccm + 400 sccm (100 sccm through every hollow cathode)
Web tension	450 N
HMDSO flow	125 sccm
Oxygen flow	250–2000 sccm
HC discharge current/voltage	100 and 131 A/24–26 V
BA discharge current/voltage	17 and 33 A/7–16 and 17–22 V

the transmission spectra in SCOUT. The dynamic deposition rates were calculated by multiplying the film thickness by the web speed.

The Water Vapor Transmission Rate (WVTR) was measured using a WDDG Water Vapor Permeability Tester made by Brugger. The extrinsic WVTR was measured over an area of 80 cm^2 at 38 °C and 90% r.h.

XPS Measurements were performed to obtain information about the chemical composition Surface contamination was removed from the samples by etching 3 nm away using an argon plasma. After etching, XPS measurements were performed using a 12 kV Mg-Kα X-Ray beam and a Phoibos 100 MCD hemispherical analyzer. An additional measurement was made at 10 nm depth to check for chemical gradients in the film.

FTIR analysis was done to obtain information about the chemical bonding. For the FTIR analysis, samples were reproduced on an identical PET film with a thick aluminium coating which was used as an IR-mirror. The bare mirror on PET was measured to make sure that the PET substrate did not influence the FTIR measurements. The measurements were performed using a Spectrum 2000 FTIR Spectrometer (Perkin Elmer).

XRR was used measure the mass density of the deposited coatings. The measurement was performed using a Bruker D8 Discover. The simulation of the measured curves was performed using GenX [22]. The XPS results were used to relate the measured electron density to the mass density. For more information reference is made to Stoev [23].

SEM was performed to obtain information about the surface morphology. An SU8000 (Hitachi) was used in SE + BSE(U) detection mode. An acceleration voltage of 0.5 kV was used to avoid damaging of the samples.

3. Results and discussion

3.1. Thickness and deposition rates

Earlier results showed that the deposition geometry used is able to deposit polymeric layers with dynamic deposition rates up to 3000 nm ∗ m/min [19]. In this research, substantially lower HMDSO and O_2 flows were used to increase the applied power per unit of monomer. A coating thickness between 320 and 360 nm was measured for the samples deposited in the low power mode and between 400 and 460 nm in the high power mode as shown in Fig. 2. Because the web speed was set at 1 m/min for all samples. The dynamic deposition rates, given in nm ∗ m/min, equal the calculated film thickness. Even though this is substantially lower compared to the polymeric layers, these functional layers are still deposited with much higher deposition rates (>8 times faster) compared to magnetron sputtering (indicated by the blue triangle). The analyzed SiO_2 layer was deposited with a coating speed of 0.13 m/min. Therefore, the dynamic deposition rate does
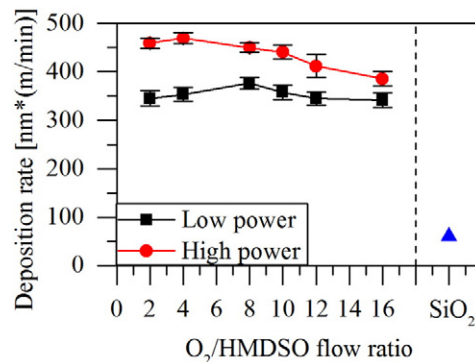

Fig. 2. Deposition rates of the arcPECVD process. The squares represent the sample made with a low current and the dos the high current. The blue triangle is the deposition rate of reactive magnetron sputtering and is given as a comparison.

not equal the coating thickness. A slight decrease in the deposition rate was found for higher oxygen flows. This was assigned to an increased etching effect due to oxygen impingements [24].

3.2. Barrier properties

The measured Water Vapor Transmission rates (WVTRs) are shown in Fig. 3. On the left and right side of the figure, the WVTR of the bare substrate and the WVTR of the sputtered SiO_2 coating are given (blue triangles). The coatings deposited in the low power mode (black squares) show no significant decrease of the WVTR whereas a significant trend is visible for the samples deposited in the high power mode (red dots). Where the literature shows that the WVTR usually decreases with an increase in the oxygen content [2,14,15], these results show an opposite trend. The 500 nm thick PECVD deposited layer with a low oxygen flow, which was produced with a web speed of 1 m/min, approaches the barrier performance of the 150 nm sputtered SiO_2 layer with a WVTR of 0.16 g/(m^2 day). This corresponds to a barrier improvement factor of 50 compared to the PET substrate. The latter one was produced with a web speed of 0.13 m/min. The layers with a higher oxygen over HMDSO show a higher WVTR which for Oxygen/HMDSO = 16 approaches the WVTR of the PET film.

This unexpected change is assigned to the current driven power supply. The voltages that were applied for the different samples, in order to reach the set point current, were measured and are shown in Fig. 4. For the low power mode, the applied voltage is practically independent of the oxygen flow. However, in the high power mode, a lower voltage is applied to obtain the same current for higher oxygen flows. This is a result of the higher pressure that increases conductivity of the plasma. For the oxygen to HMDSO ratio of 16, the applied voltage is approximately the same to the measured voltage during low power deposition. This is a drastic decrease of the applied power (up to 50% compared to the flow ratio of 2).

3.3. Chemical composition

The chemical composition was measured using XPS. For all samples, measurements were made after removing 3 and 10 nm, respectively. Both measurements showed similar compositions (± 1 at%) which indicates that there are no significant chemical gradients at the interface of the sample. Fig. 5 shows the average values of the two measurements of the coatings that were deposited in higher power mode. It should be mentioned that of course this value only represents the first 15 nm of the deposited layer. However, Glow Discharge-Optical Emission Spectroscopy (GD-OES) measurements indicate that the chemical composition does not change significantly as a function of the coating depth.

With high power and low oxygen flow, the content of carbon exceeds that of the silicon or oxygen whereas for high power and high
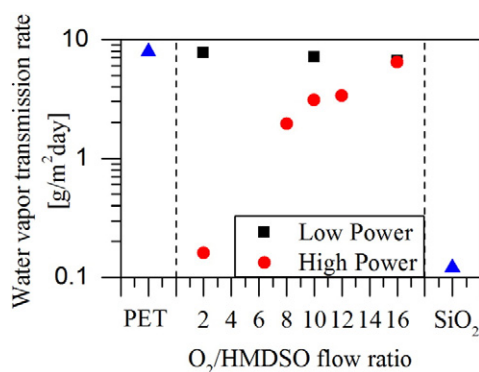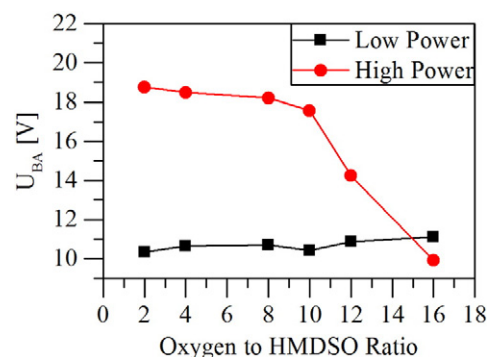
Fig. 4. The applied booster anode voltage which was measured during the deposition of the thin film coatings.

oxygen flows, the carbon content reduces drastically. This indicates that the increased oxygen flow lowers the carbon content as a result of methyl extraction [25] and replacement by oxygen bonds. A small amount of carbon (4–5 at%) is measured which is similar to that of the sputtered SiO_2 layer. The silicon content is about stable.

3.4. Mass density

Fig. 6 shows the results of the density measurement. Due to the lack of information about the hydrogen content, an error is introduced in the density calculations. Calculations with different amounts of hydrogen however showed that this influence is less than 0.08 g/cm^3. This is due to the low molar weight of hydrogen. The mass density shown in Fig. 6 is calculated under the assumption that no hydrogen is present in the thin films. This results in a slight overestimation of the calculated density. The error upwards is mainly a result of the mismatch between fit and measurement. The bulk density is clearly increasing with increasing oxygen content and approaches the density of sputtered SiO_2. These results are in good agreement with the observations from other authors (e.g. Agres et al. [26]). They observed that, for an RF plasma, the density increased with increasing oxygen flow.

3.5. FTIR spectroscopy

Fig. 7 shows the FTIR (Fourier-transformed infrared spectra) of the coatings. Significant difference is found in chemical bonds between the PECVD coated samples with high and low oxygen flow but also between the PECVD coated sample with high oxygen flow and the sputtered SiO_2 layer. The high peak doublet at 2340 and 2360 cm^1 is caused by CO_2 [27] and was a result of the CO_2 present in the measurement chamber. The peaks at 840 and 800 cm^{-1} are assigned to $Si(CH_3)_3$ and $Si(CH_3)_2$ rocking oscillations, respectively. The peaks at 2913 and

Fig. 3. Water Vapor Transmission rates of the deposited samples. The data point of the left represents the WVTR for bare PET whereas the most right data point represent the WVTR for the sputtered SiO_2.
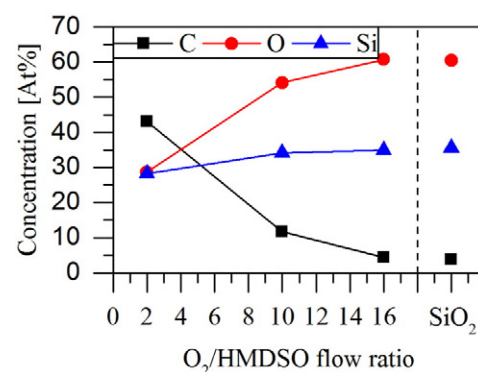
Fig. 5. This figure shows the results of the XPS measurements of the samples made in high power mode. The values shown are averaged values of the measurements at 5 and 10 nm depth.
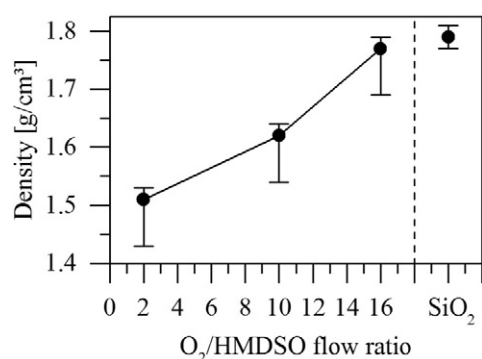
Fig. 6. The density of the coatings produced with higher power as calculated by XRR.

2966 cm^{-1} cm are assigned to asymmetric and symmetric stretching of CH$_3$ [28]. The maximum intensity of these peaks decreases with increasing oxygen flow. This indicates a reduction of CH$_x$ groups in the layers with increasing O$_2$ flow. This also agrees with the decrease of carbon as shown by XPS. The large peak from 3000 to 3750 cm^{-1} is assigned to OH groups within the plasma polymer films [29]. Neither CH$_3$ nor OH groups are observed in the sputtered sample. The number of OH groups, however, increases with increasing oxygen flow but decreases again for an oxygen over HMDSO ratio of 16. The peak between 2260 and 2095 cm^{-1} can be assigned to Si—H bonds [30]. A small amount of Si—H bonds was observed for the coating with low oxygen flow whereas no peaks were found for the samples with higher oxygen flow.

Between 1000 and 1250 cm^{-1}, the sputtered SiO$_2$ film shows only two significant peaks at 1235 and 1050 cm^{-1}. These peaks are assigned to longitudinal optical phonon and transverse optical phonon mode in an Si—O stretch, respectively [11,31]. The PECVD samples show an overlapped peak. Deconvolution using two Gaussian peaks was performed to analyze the peaks. For increasing oxygen flow, the right peak slowly shifts from 1006 cm^{-1} to 1042 cm^{-1} whereas the left peak shifts from 1086 cm^{-1} to 1150 cm^{-1}. Meanwhile, the intensity of the left peak increases compared to the intensity of the right peak. Pai et al. [32] also observed these peaks. He designated the left peak as a broad shoulder which increases with increasing oxygen content. The shift was related to the oxygen to silicon ratio. With less oxygen, other bonds than Si—O are formed, which result in a shift of the Si-O-Si frequency. The broadening is a result of the increase in different bonding arrangements that are present within the coating. The different angles agree with the presence of (Si-O)$_n$ ring structure [33]. Densification of the coating by e.g. ion bombardment reduces the average size of the rings which results in a shift of the peak. The lack of barrier performance of the SiO$_2$ like PECVD layer was explained by the presence of CH$_x$ and OH groups as well as presence of (Si-O)$_n$ rings. The single bond of

hydrogen reduces the cross-linking of the plasma polymer which results in a lower density as compared to the sputtered SiO$_2$ coating whereas the larger rings create preferred permeation pathways.

The existence of barrier performance for the sample with low oxygen flow was explained by Weston [34]. The explanation was based on the idea that (Si-O)$_n$ rings, which are preferred permeation pathways, are filled up by carbon atoms. This would lead to a more dense structure and increased cross-linking and would explain the decreasing WVTR with increasing carbon content. It should be mentioned that the explanations given for the change in chemical composition are based on simplified models that can give the reader an idea about the structure of the coating. In reality, the exact structure is far too complex and consists of a wide variety of different bonds to a higher or lesser degree.

3.6. SEM

The samples deposited in high power mode with both high and low oxygen gas flow were analyzed using electron microscopy. Also the reference coating was analyzed. The images are shown in Fig. 8. All samples show a smooth surface up to higher magnification were the commonly known cauliflower-like structure was observed. The microstructure of the sputtered coating shows major differences compared to the sputtered coatings. The sputtered coatings shows a high density film with small semispherical features on the surface. Both PECVD coatings show a columnar structure were small columns are packed together in a cauli-flower like structure. The deeper pores in the SiO$_2$-like coating are an indication that the molecules are not close packed enough to perform as a good water permeation barrier. However, it is difficult to make quantitative conclusions based on the images. No cracking of the coatings was observed.

4. Conclusions

Silicon containing plasma polymer layers were deposited using a hollow cathode arc discharge plasma with a variety of oxygen to HMDSO ratios with excellent deposition rates up to 500 nm ∗ m/min. The permeation barrier performance, chemical, density and microstructural properties were examined and compared to those of a SiO$_2$ layer which was deposited using reactive dual magnetron sputtering. It was found that for a high oxygen flow, the sample shows similar characteristics regarding chemical composition. However, it showed a slightly lower density. SEM confirmed the less dense structure of the PECVD coatings compared to the sputtered SiO$_2$ coating. FTIR shows differences in the chemical bonding compared to the SiO$_2$ layer. However the barrier performance against water was found to be approaching the value of the PET substrate. The organic sample with low oxygen flow, however, shows a WVTR of 0.16 g/m^2 day which approaches the value of the SiO$_2$ layer. Since the organic plasma polymer layer shows almost no
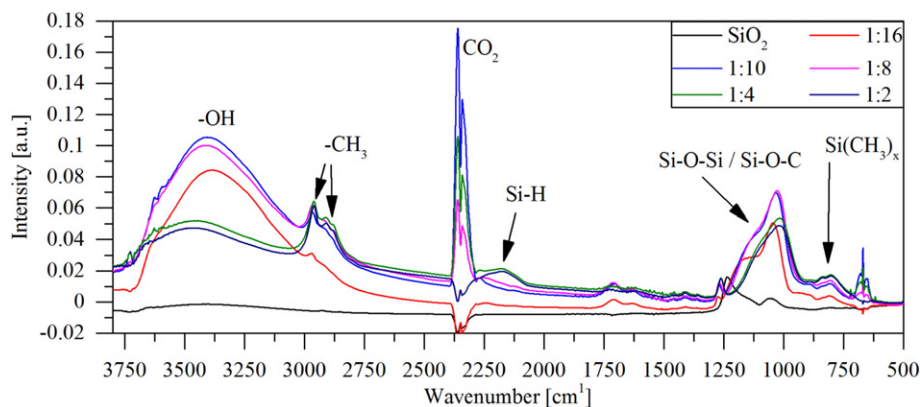

Fig. 7. Fourier transformed infrared spectrum of the plasma polymer layers made in high power mode. The black line shows the sputtered SiO$_2$ spectrum. The ratio in the legend represents the oxygen to HMDSO ratio for the PECVD samples.
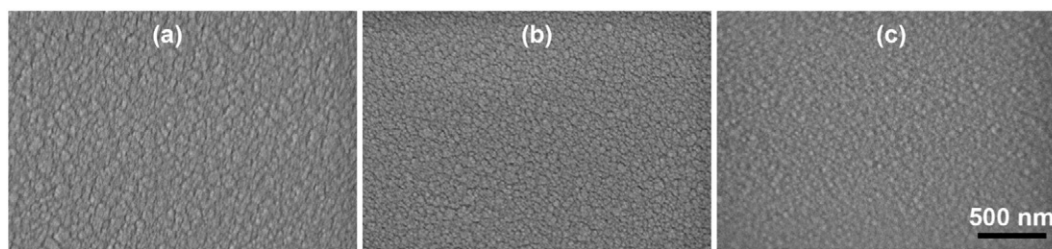
Fig. 8. SEM images of the PECVD coating in high power mode with (a) low oxygen flow, (b) high oxygen flow and (c) the sputtered reference coating.

similarities compared to the SiO$_2$ layer. The inclusion of hydrogen containing groups (OH, CH$_x$) in the film, as well as the (Si-O)$_n$ rings lower the density which results in an increased WVTR. Including sufficient carbon, however, leads to an improvement barrier performance as a result of filling of the preferred permeation pathways.

It was also shown that a current regulated hollow cathode PECVD process can be used to control the chemical composition of the thin films. However, for the deposition of barrier films, the applied power as well as the carbon content are crucial to accurately control the thin film properties.

Acknowledgements

References

[1] W. Huang, X. Wang, M. Sheng, L. Xu, F. Stubhan, L. Luo, T. Feng, F. Zhang, S. Zou, Low temperature PECVD SiNx films applied in OLED packaging, Mater. Sci. Eng. B 98 (2003) 248–254.

[2] A. Bieder, A. Gruniger, R. von Rohr, Deposition of SiOx diffusion barriers on flexible packaging materials by PECVD, Surf. Coat. Technol. 200 (2005) 928–931.

[3] J. Madocks, J. Rewhinkle, L. Barton, Packaging barrier films deposited on PET by PECVD using a new high density plasma source, Mater. Sci. Eng. B 119 (2005) 268–273.

[4] M. Deilmann, H. Halfmann, S. Steves, N. Bibinov, P. Awakowicz, Silicon oxide permeation barrier coating and plasma sterilization of PET bottles and foils, Plasma Process. Polym. 6 (2009) 695–699.

[5] H. Morgner, M. Neumann, S. Straach, M. Krug, The hollow cathode: a high-performance tool for plasma-activated deposition, Surf. Coat. Technol. 108–109 (1998) 513–519.

[6] J. Fahlteich, W. Schönberger, M. Fahland, N. Schiller, Characterization of reactively sputtered permeation barrier materials on polymer substrates, Surf. Coat. Technol. 205 (2011) 141–144.

[7] P.V. Mercea, M. Bârţan, The permeation of gases through a poly (ethylene terephthalate) membrane deposited with SiO2, J. Membr. Sci. 59 (1991) 353–358.

[8] A. Patelli, S. Vezzù, L. Zottarel, E. Menin, C. Sada, A. Martucci, S. Costacurta, SiOx-based multilayer barrier coatings produced by a single PECVD process, Plasma Process. Polym. 6 (2009) 665–670.

[9] A.G. Erlat, M. Yan, T.W. Kim, M. Schaepkens, J. Liu, C.M. Heller, McConnelee, 48th Annual Technical Conference Proceedings of the Society of Vacuum Coaters, 2005 116–120.

[10] S. Zanini, C. Riccardi, M. Orlandi, E. Grimoldi, Characterisation of SiOxCyHz thin films deposited by low-temperature PECVD, Vacuum 82 (2007) 290–293.

[11] J.D. Ferguson, E.R. Smith, A.W. Weimer, S.M. George, ALD of SiO2 at room temperature using TEOS and H2O with NH3 as the catalyst, J. Electrochem. Soc. 151 (2004) 528–535.

[12] M. Komada, T. Oboshi, K. Ichimura, Proceedings of the 43th Annual Technical Conference of the Society of Vacuum Coaters, 2000 352–356.

[13] A. Maria Coclite, F. de Luca, K.K. Gleason, Mechanically robust silica-like coatings deposited by microwave plasmas for barrier applications, J. Vac. Sci. Technol. A 30 (2012) 61502.

[14] S. Steves, B. Ozkaya, C.-N. Liu, O. Ozcan, N. Bibinov, G. Grundmeier, P. Awakowicz, Silicon oxide barrier films deposited on PET foils in pulsed plasmas: influence of substrate bias on deposition process and film properties, J. Phys. D. Appl. Phys. 46 (2013) 84013.

[15] J. Fahlteich, Transparente Hochbarriereschichten auf flexiblen Substraten, Chemnitz, 2010.

[16] A. Mackova, V. Perina, Z. Stryhal, J. Pavlik, M. Svec, A. Quédé, P. Supiot, G. Borvon, A. Granier, P. Raynaud, The combined study of the organosilicon films by RBS, ERDA and AFM analytical methods obtained from PECVD and PACVD, Surf. Sci. 566–568 (Part 2) (2004) 1143–1146.

[17] P. Supiot, C. Vivien, A. Granier, A. Bousquet, A. Mackova, D. Escaich, R. Clergereaux, P. Raynaud, Z. Stryhal, J. Pavlik, Growth and modification of organosilicon films in PECVD and remote afterglow reactors, Plasma Process. Polym. 3 (2006) 100–109.

[18] A. Bousquet, V. Bursikova, A. Goullet, A. Djouadi, L. Zajickova, A. Granier, Comparison of structure and mechanical properties of SiO2-like films deposited in O2/HMDSO pulsed and continuous plasmas, Surf. Coat. Technol. 200 (2006) 6517–6521.

[19] S. Günther, M. Fahland, J. Fahlteich, B. Meyer, S. Straach, N. Schiller, High rate low pressure plasma-enhanced chemical vapor deposition for barrier and optical coatings, Thin Solid Films 532 (2013) 44–49.

[20] J. Fahlteich, M. Fahland, S. Straach, S. Günther, N. Schiller, Transparente Barriereschichten auf flexiblen Polymersubstraten, Vakuum in Forschung und Praxis 23 (2011) 29–37.

[21] J. Fahlteich, M. Fahland, W. Schönberger, N. Schiller, Permeation barrier properties of thin oxide films on flexible polymer substrates, Thin Solid Films 517 (2009) 3075–3080.

[22] M. Björck, G. Andersson, GenX: an extensible X-ray reflectivity refinement program utilizing differential evolution, J. Appl. Crystallogr. 40 (2007) 1174–1178.

[23] K.N. Stoev, K. Sakurai, Review on grazing incidence X-ray spectrometry and reflectometry, Spectrochim. Acta, Part B 54 (1999) 41–82.

[24] K. Li, O. Gabriel, J. Meichsner, Fourier transform infrared spectroscopy study of molecular structure formation in thin films during hexamethyldisiloxane decomposition in low pressure RF discharge, J. Phys. D. Appl. Phys. 37 (2004) 588.

[25] N.E. Blanchard, B. Hanselmann, J. Drosten, M. Heuberger, D. Hegemann, Densification and hydration of HMDSO plasma polymers, Plasma Process. Polym. 12 (2015) 32–41.

[26] L. Agres, Y. Ségui, R. Delsol, P. Raynaud, Oxygen barrier efficiency of hexamethyldisiloxane/oxygen plasma-deposited coating, J. Appl. Polym. Sci. 61 (1996) 2015–2022.

[27] A. Oancea, O. Grasset, E. Le Menn, O. Bollengier, L. Bezacier, S. Le Mouélic, G. Tobie, Laboratory infrared reflection spectrum of carbon dioxide clathrate hydrates for astrophysical remote sensing applications, Icarus 221 (2012) 900–910.

[28] D. Magni, C. Deschenaux, C. Hollenstein, A. Creatore, P. Fayet, Oxygen diluted hexamethyldisiloxane plasmas investigated by means of in situ infrared absorption spectroscopy and mass spectrometry, J. Phys. D. Appl. Phys. 34 (2001) 87–94.

[29] R. Reuter, K. Rügner, D. Ellerweg, T. de los Arcos, A. von Keudell, J. Benedikt, The role of oxygen and surface reactions in the deposition of silicon oxide like films from HMDSO at atmospheric pressure, Plasma Process. Polym. 9 (2012) 1116–1124.

[30] S. Holly, P. Sohár, L. Láng, Absorption Spectra in the Infrared Region, Akadémiai Kiadó, Budapest, 1977.

[31] B.B. Burton, S.W. Kang, S.W. Rhee, S.M. George, SiO2 atomic layer deposition using tris(dimethylamino)silane and hydrogen peroxide studied by in situ transmission FTIR spectroscopy, J. Phys. Chem. C 113 (2009) 8249–8257.

[32] P.G. Pai, Infrared spectroscopic study of SiOx films produced by plasma enhanced chemical vapor deposition, J. Vac. Sci. Technol. A 4 (1986) 689.

[33] A. Lefèvre, L.J. Lewis, L. Martinu, M.R. Wertheimer, Structural properties of silicon dioxide thin films densified by medium-energy particles, Phys. Rev. B 64 (2001) 115429.

[34] G.F. Weston, A paper in our education series: the theory and practice of vacuum science and technology in schools and colleges, Vacuum 25 (1975) 469–484.